1-1-2008

Measurement of ep→epπ0 beam spin asymmetries above the resonance region

R. DeMasi

Angela Biselli
Fairfield University, abiselli@fairfield.edu

CLAS Collaboration

Peer Reviewed

Published Citation

R. De Masi et al. [CLAS Collaboration], "Measurement of ep→epπ0 beam spin asymmetries above the resonance region", Physical Review C 77.4 (2008) DOI: 10.1103/PhysRevC.77.042201

PHYSICAL REVIEW C **70**, 042201(R) (2004)

Measurement of the polarized structure function $\sigma_{LT'}$ for $p(\vec{e},e'\pi^+)n$ in the $\Delta(1232)$ resonance region

K. Joo,[1] L. C. Smith,[2] I. G. Aznauryan,[40] V. D. Burkert,[3] R. Minehart,[2] G. Adams,[33] P. Ambrozewicz,[12] E. Anciant,[5] M. Anghinolfi,[18] B. Asavapibhop,[25] G. Asryan,[40] G. Audit,[5] T. Auger,[5] H. Avakian,[3,17] H. Bagdasaryan,[30] J. P. Ball,[4] S. Barrow,[13] V. Batourine,[23] M. Battaglieri,[18] K. Beard,[22] M. Bektasoglu,[29,30,*] N. Benmouna,[15] N. Bianchi,[17] A. S. Biselli,[7] S. Boiarinov,[3,21] B. E. Bonner,[34] S. Bouchigny,[20] R. Bradford,[7] D. Branford,[11] W. J. Briscoe,[15] W. K. Brooks,[3] S. Bültmann,[30] C. Butuceanu,[39] J. R. Calarco,[27] D. S. Carman,[29] B. Carnahan,[8] C. Cetina,[7,15] S. Chen,[13] L. Ciciani,[30] P. L. Cole,[19,3] D. Cords,[3,†] P. Corvisiero,[18] D. Crabb,[2] H. Crannell,[8] J. P. Cummings,[33] E. De Sanctis,[17] R. DeVita,[18] P. V. Degtyarenko,[3] L. Dennis,[13] A. Deur,[3] K. V. Dharmawardane,[30] K. S. Dhuga,[15] C. Djalali,[36] G. E. Dodge,[30] D. Doughty,[9,3] P. Dragovitsch,[13] M. Dugger,[4] S. Dytman,[32] O. P. Dzyubak,[36] H. Egiyan,[3] K. S. Egiyan,[40] L. Elouadrhiri,[3,9] A. Empl,[33] P. Eugenio,[13] R. Fersch,[39] R. J. Feuerbach,[3] T. A. Forest,[30] H. Funsten,[39] S. J. Gaff,[10] M. Garçon,[5] G. Gavalian,[27,40] S. Gilad,[24] G. P. Gilfoyle,[35] K. L. Giovanetti,[22] R. W. Gothe,[36] K. A. Griffioen,[39] M. Guidal,[20] M. Guillo,[36] N. Guler,[30] L. Guo,[3] V. Gyurjyan,[3] C. Hadjidakis,[20] R. S. Hakobyan,[8] J. Hardie,[9] D. Heddle,[9,3] F. W. Hersman,[27] K. Hicks,[29] I. Hleiqawi,[29] M. Holtrop,[27] J. Hu,[33] C. E. Hyde-Wright,[30] Y. Ilieva,[15] D. Ireland,[16] M. M. Ito,[3] D. Jenkins,[38] H. G. Juengst,[15] J. D. Kellie,[16] J. H. Kelley,[10] M. Khandaker,[28] K. Y. Kim,[32] K. Kim,[23] W. Kim,[23] A. Klein,[30] F. J. Klein,[8,3] A. V. Klimenko,[30] M. Klusman,[33] M. Kossov,[21] V. Koubarovski,[33] L. H. Kramer,[12,3] S. E. Kuhn,[30] J. Kuhn,[7] J. Lachniet,[7] J. M. Laget,[5] J. Langheinrich,[36] D. Lawrence,[25] T. Lee,[27] K. Livingston,[16] K. Lukashin,[8,3] J. J. Manak,[3] C. Marchand,[5] S. McAleer,[13] J. W. C. McNabb,[31] B. A. Mecking,[3] M. D. Mestayer,[3] C. A. Meyer,[7] K. Mikhailov,[21] M. Mirazita,[17] R. Miskimen,[25] V. Mokeev,[26] L. Morand,[5] S. A. Morrow,[5,20] V. Muccifora,[17] J. Mueller,[32] G. S. Mutchler,[34] J. Napolitano,[33] R. Nasseripour,[12] S. O. Nelson,[10] S. Niccolai,[20] G. Niculescu,[22,29] I. Niculescu,[22,15] B. B. Niczyporuk,[3] R. A. Niyazov,[3,30] M. Nozar,[3] G. V. O'Rielly,[15] M. Osipenko,[18] A. I. Ostrovidov,[13] K. Park,[23] E. Pasyuk,[4] G. Peterson,[25] S. A. Philips,[15] N. Pivnyuk,[21] D. Pocanic,[2] O. Pogorelko,[21] E. Polli,[17] S. Pozdniakov,[21] B. M. Preedom,[36] J. W. Price,[6] Y. Prok,[2] D. Protopopescu,[16] L. M. Qin,[30] B. A. Raue,[12] G. Riccardi,[13] G. Ricco,[18] M. Ripani,[18] B. G. Ritchie,[4] F. Ronchetti,[17] G. Rosner,[16] P. Rossi,[17] D. Rowntree,[25] P. D. Rubin,[35] F. Sabatié,[5] K. Sabourov,[10] C. Salgado,[28] J. P. Santoro,[38] V. Sapunenko,[3,18] R. A. Schumacher,[7] V. S. Serov,[21] Y. G. Sharabian,[3,40] J. Shaw,[25] S. Simionatto,[15] A. V. Skabelin,[24] E. S. Smith,[3] D. I. Sober,[8] M. Spraker,[10] A. Stavinsky,[21] S. Stepanyan,[3] S. S. Stepanyan,[23] B. E. Stokes,[13] P. Stoler,[33] I. I. Strakovsky,[15] S. Strauch,[15] M. Taiuti,[18] S. Taylor,[34] D. J. Tedeschi,[36] U. Thoma,[14,3] R. Thompson,[32] A. Tkabladze,[29] L. Todor,[35] C. Tur,[36] M. Ungaro,[1] M. F. Vineyard,[37] A. V. Vlassov,[21] K. Wang,[2] L. B. Weinstein,[30] H. Weller,[10] D. P. Weygand,[3] M. Williams,[7] E. Wolin,[3] M. H. Wood,[36] A. Yegneswaran,[3] J. Yun,[30] L. Zana,[27] and The CLAS Collaboration

[1]*University of Connecticut, Storrs, Connecticut 06269, USA*
[2]*University of Virginia, Charlottesville, Virginia 22901, USA*
[3]*Thomas Jefferson National Accelerator Facility, Newport News, Virginia 23606, USA*
[4]*Arizona State University, Tempe, Arizona 85287-1504, USA*
[5]*CEA-Saclay, Service de Physique Nucléaire, F91191 Gif-sur-Yvette, Cedex, France*
[6]*University of California at Los Angeles, Los Angeles, California 90095-1547, USA*
[7]*Carnegie Mellon University, Pittsburgh, Pennsylvania 15213, USA*
[8]*Catholic University of America, Washington, D.C. 20064, USA*
[9]*Christopher Newport University, Newport News, Virginia 23606, USA*
[10]*Duke University, Durham, North Carolina 27708-0305, USA*
[11]*Edinburgh University, Edinburgh EH9 3JZ, United Kingdom*
[12]*Florida International University, Miami, Florida 33199, USA*
[13]*Florida State University, Tallahassee, Florida 32306, USA*
[14]*Physikalisches Institut der Universitaet Giessen, 35392 Giessen, Germany*
[15]*The George Washington University, Washington, D.C. 20052, USA*
[16]*University of Glasgow, Glasgow G12 8QQ, United Kingdom*
[17]*INFN, Laboratori Nazionali di Frascati, Frascati, Italy*
[18]*INFN, Sezione di Genova, 16146 Genova, Italy*
[19]*Idaho State University, Pocatello, Idaho 83209, USA*
[20]*Institut de Physique Nucleaire ORSAY, Orsay, France*
[21]*Institute of Theoretical and Experimental Physics, Moscow, 117259, Russia*
[22]*James Madison University, Harrisonburg, Virginia 22807, USA*
[23]*Kungpook National University, Taegu 702-701, South Korea*
[24]*Massachusetts Institute of Technology, Cambridge, Massachusetts 02139-4307, USA*
[25]*University of Massachusetts, Amherst, Massachusetts 01003, USA*
[26]*Moscow State University, General Nuclear Physics Institute, 119899 Moscow, Russia*
[27]*University of New Hampshire, Durham, New Hampshire 03824-3568, USA*
[28]*Norfolk State University, Norfolk, Virginia 23504, USA*

[29]*Ohio University, Athens, Ohio 45701, USA*
[30]*Old Dominion University, Norfolk, Virginia 23529, USA*
[31]*Penn State University, University Park, Pennsylvania 16802, USA*
[32]*University of Pittsburgh, Pittsburgh, Pennsylvania 15260, USA*
[33]*Rensselaer Polytechnic Institute, Troy, New York 12180-3590, USA*
[34]*Rice University, Houston, Texas 77005-1892, USA*
[35]*University of Richmond, Richmond, Virginia 23173, USA*
[36]*University of South Carolina, Columbia, South Carolina 29208, USA*
[37]*Union College, Schenectady, New York 12308, USA*
[38]*Virginia Polytechnic Institute and State University, Blacksburg, Virginia 24061-0435, USA*
[39]*College of William and Mary, Williamsburg, Virginia 23187-8795, USA*
[40]*Yerevan Physics Institute, 375036 Yerevan, Armenia*
(Received 15 July 2004; published 25 October 2004)

The polarized longitudinal-transverse structure function $\sigma_{LT'}$ has been measured using the $p(\vec{e},e'\pi^+)n$ reaction in the $\Delta(1232)$ resonance region at $Q^2=0.40$ and 0.65 GeV^2. No previous $\sigma_{LT'}$ data exist for this reaction channel. The kinematically complete experiment was performed at the Jefferson Lab with the CEBAF large acceptance spectrometer using longitudinally polarized electrons at an energy of 1.515 GeV. A partial-wave analysis of the data shows generally better agreement with recent phenomenological models of pion electroproduction compared to the previously measured π^0p channel. A fit to both π^0p and π^+n channels using a unitary isobar model suggests the unitarized Born terms provide a consistent description of the nonresonant background. The *t*-channel pion pole term is important in the π^0p channel through a rescattering correction, which could be model dependent.

DOI: 10.1103/PhysRevC.70.042201 PACS number(s): 13.60.Le, 12.40.Nn, 13.40.Gp

The excitation of nucleon resonances using electromagnetic interactions is an essential tool for understanding quark confinement. However, the excited states of the nucleon decay rapidly through the emission of mesons. Thus, the resonance formation mechanism can involve both hadronic structure and reaction dynamics, intermixing quark and meson degrees of freedom. To understand the role of the meson cloud in resonance photoexcitation, a variety of theoretical approaches have been developed, e.g., chiral quark and soliton models, chiral perturbation theory, dispersion relations, effective Lagrangian and dynamical models, and most recently, lattice QCD.

A unique generation of high-precision photoproduction and electroproduction experiments have made it possible to test theoretical predictions with unprecedented accuracy. The most precise measurements exist for excitation energies around the $\Delta(1232)$ resonance and four-momentum transfers $Q^2<1$ GeV^2. Experiments using polarized real photons at LEGS and Mainz [1,2] and unpolarized electrons at Bates, ELSA, and the Thomas Jefferson National Accelerator Facility (Jefferson Lab) [3–6] have measured $\Delta^+\rightarrow p\pi^0$ decay angular distributions with the goal of determining the magnitude and Q^2 evolution of the $N\Delta$ transition photocoupling amplitudes. However, theoretical calculations predict a substantial modification of the $N\Delta$ form factors due to the presence of nonresonant Born diagrams (Fig. 1). Moreover, these predictions are subject to considerable model dependence from the treatment of πN rescattering in the final state.

To better study these nonresonant contributions, several recent $p(\vec{e},e'p)\pi^0$ experiments in the $\Delta(1232)$ region [7–12] have utilized single spin-polarization observables to directly determine the imaginary part of interfering amplitudes. In this way, the nonresonant amplitudes, which are largely real, are greatly amplified by the imaginary part of the dominant $\Delta(1232)$ $M_{1+}^{3/2}$ resonant multipole. Until now, beam asymmetry measurements existed only for the π^0p channel, where pion rescattering corrections are large and model dependent [13,14]. Predictions for the π^+n channel show less model dependence, and are dominated by the *t*-channel pion pole and contact Born terms, which are absent or weak in the π^0p channel. Measurement of both charge channels is therefore essential to test the consistency of the model descriptions.

We present measurements of the longitudinal-transverse polarized structure function $\sigma_{LT'}$ obtained in the $\Delta(1232)$ resonance region using the $p(\vec{e},e'\pi^+)n$ reaction. The data reported here span the invariant-mass interval $W=1.1-1.3$ GeV at $Q^2=0.40$ and 0.65 GeV^2, and cover the full angular range in the π^+n center of mass (c.m.). These data were taken simultaneously with the $p(\vec{e},e'p)\pi^0$ channel for which results were reported previously [12].

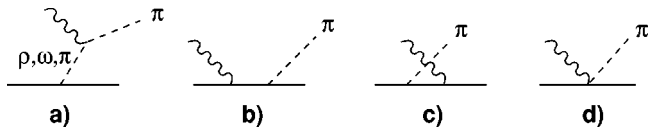

FIG. 1. Born terms which contribute to nonresonant background in π electroproduction: (a) *t*-channel pseudoscalar and vector meson exchange, (b) *s*-channel nucleon pole, (c) *u*-channel nucleon pole, and (d) contact term.

*Current address: Sakarya University, Sakarya, Turkey.
†Deceased.

The experiment was performed at the Jefferson Lab using a 1.515 GeV, 100% duty-cycle beam of longitudinally polarized electrons incident on a liquid-hydrogen target. The electron polarization was determined by Møller polarimeter measurements to be $0.690 \pm 0.009(\text{stat.}) \pm 0.013(\text{syst.})$. Scattered electrons and pions were detected in the CEBAF large acceptance spectrometer (CLAS) [15]. Electron triggers were enabled through a hardware coincidence of the gas Čerenkov counters and the lead-scintillator electromagnetic calorimeters. Particle identification was accomplished using momentum reconstruction in the tracking system and time of flight from the target to the scintillators. Software fiducial cuts were used to exclude regions of nonuniform detector response. Kinematic corrections were applied to compensate for drift chamber misalignments and uncertainties in the magnetic field. The $\pi^+ n$ final state was identified using a 2σ cut on the missing neutron mass. Target window backgrounds were suppressed with cuts on the reconstructed $e'\pi^+$ target vertex.

The single-pion electroproduction cross section is given by

$$\frac{d^4\sigma^h}{dQ^2 dW d\Omega_\pi^*} = J\,\Gamma_v \frac{d^2\sigma^h}{d\Omega_\pi^*}, \tag{1}$$

where Γ_v is the virtual-photon flux and the Jacobian $J = \partial(Q^2, W)/\partial(E', \cos\theta_e, \phi_e)$ relates the differential volume element $dQ^2 dW$ of the binned data to the measured electron kinematics $dE'\, d\cos\theta_e\, d\phi_e$. Here $d^2\sigma^h$ is the c.m. differential cross section for $\gamma^* p \to n\pi^+$ with electron-beam helicity ($h = \pm 1$). For an unpolarized target $d^2\sigma^h$ depends on the transverse ϵ and longitudinal ϵ_L polarization of the virtual photon through five structure functions: $\sigma_T, \sigma_L, \sigma_{TT}$, and the transverse-longitudinal interference terms σ_{LT} and $\sigma_{LT'}$,

$$\frac{d^2\sigma^h}{d\Omega_\pi^*} = \frac{p_\pi^*}{k_\gamma^*}[\sigma_0 + h\sqrt{2\epsilon_L(1-\epsilon)}\,\sigma_{LT'} \sin\theta_\pi^* \sin\phi_\pi^*],$$

$$\sigma_0 = \sigma_T + \epsilon_L\sigma_L + \epsilon\,\sigma_{TT}\sin^2\theta_\pi^* \cos 2\phi_\pi^* + \sqrt{2\epsilon_L(1+\epsilon)}\,\sigma_{LT}\sin\theta_\pi^*\cos\phi_\pi^*, \tag{2}$$

where p_π^* and θ_π^* are the π^+ c.m. momentum and polar angle, ϕ_π^* is the azimuthal rotation of the hadronic plane with respect to the electron-scattering plane, $\epsilon = (1 + 2|\vec{q}|^2 \tan^2(\theta_e/2)/Q^2)^{-1}$, $\epsilon_L = (Q^2/|k^*|^2)\epsilon$, $|k^*|$ is the virtual photon c.m. momentum, and k_γ^* is the real photon equivalent energy.

Determination of $\sigma_{LT'}$ was made through the asymmetry $A_{LT'}$,

$$A_{LT'} = \frac{d^2\sigma^+ - d^2\sigma^-}{d^2\sigma^+ + d^2\sigma^-} \tag{3}$$

$$= \frac{\sqrt{2\epsilon_L(1-\epsilon)}\,\sigma_{LT'}\sin\theta_\pi^*\sin\phi_\pi^*}{\sigma_0}. \tag{4}$$

The asymmetry $A_{LT'}$ was obtained for individual bins of $(Q^2, W, \cos\theta_\pi^*, \phi_\pi^*)$ by dividing the measured single spin beam asymmetry A_m by the magnitude of the electron-beam polarization P_e,

$$A_{LT'} = \frac{A_m}{P_e}, \tag{5}$$

$$A_m = \frac{N_{\pi^+} - N_{\pi^-}}{N_{\pi^+} + N_{\pi^-}}, \tag{6}$$

where $N_\pi^\pm$ is the number of detected $n\pi^+$ events for each electron-beam helicity state, normalized to beam charge. Acceptance studies which varied the sizes of all kinematic bins showed no significant helicity dependence, leaving A_m largely free from systematic errors. Radiative corrections were applied for each bin using the program recently developed by Afanasev *et al.* for exclusive pion electroproduction [16]. Corrections were also applied to compensate for cross section variations over the width of each bin, using the cross-section model MAID2000, described below. An example of the measured ϕ_π^* dependence of $A_{LT'}$ is shown in Fig. 2. Next, the $A_{LT'}$ distributions were multiplied by the unpolarized $p(e, e'\pi^+)n$ cross section σ_0, using a parametrization of measurements of σ_0 made during the same experiment [17]. The structure function $\sigma_{LT'}$ was then extracted using Eq. (4) by fitting the ϕ_π^* distributions. Systematic errors for $\sigma_{LT'}$ were dominated by uncertainties in determination of the electron-beam polarization and the parametrization of σ_0. The systematic error for A_m is negligible in comparison. Quadratic addition of the individual contributions yields a total relative systematic error of $<6\%$ for all of our measured data points.

Figure 3 shows typical c.m. angular distributions for $\sigma_{LT'}$ at $Q^2 = 0.40$ GeV^2 and $W = 1.18 - 1.26$ GeV. Our previous measurement for the $\pi^0 p$ [12] channel (top) and our new measurement for the $\pi^+ n$ channel (bottom) are shown compared to phenomenological models by Sato and Lee (SL) [18], the Dubna–Mainz–Taipei (DMT) group [19], and Drechsel *et al.* (MAID) [20]. These models combine Breit–Wigner-type resonant amplitudes with backgrounds arising from Born diagrams and t-channel vector-meson exchange, while different methods are used to satisfy unitarity. The SL and DMT models use a reaction theory to calculate the effect of off-shell πN rescattering. MAID uses a K-matrix approximation, by incorporating the πN scattering phase shifts [21] into the background amplitudes and treating the rescattered pion as on shell. All well-established resonances are included in DMT and MAID2000, whereas SL treats only the $\Delta(1232)$.

The measured angular distributions of $\sigma_{LT'}$ for the $\pi^+ n$ channel show a strong forward peaking for W bins around the $\Delta(1232)$, in contrast to the $\pi^0 p$ channel, which shows backward peaking. The calculations qualitatively describe the peaking behavior of both the π^0 and π^+ channels, which arises largely from the pion pole term (Fig. 1 and SL curves on Fig. 3), as discussed shortly. The largest variation between the models occurs in their predictions for the overall magnitude of $\sigma_{LT'}$, although the variation is substantially smaller for the $\pi^+ n$ channel.

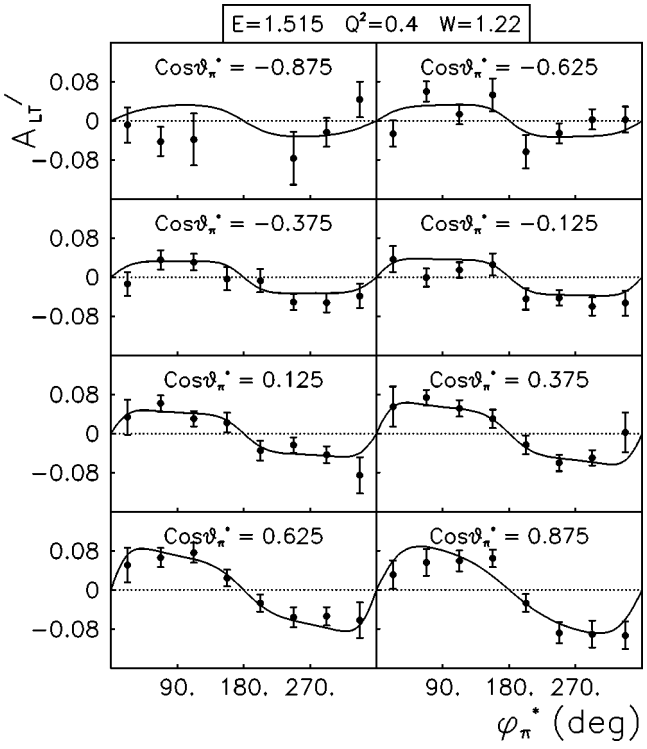

FIG. 2. CLAS measurement of the beam asymmetry $A_{LT'}$ vs ϕ_π^* for the $p(\vec{e},e'\pi^+)n$ reaction at $Q^2=0.40$ GeV^2 and $W=1.22$ GeV. Bin sizes were $\Delta Q^2=0.2$ GeV^2 and $\Delta W=0.04$ GeV. The curves show predictions from the MAID2000 model described in the text.

A more quantitative comparison was made through fitting the extracted $\sigma_{LT'}$ angular distributions using the Legendre expansion,

$$\sigma_{LT'} = D_0' + D_1' P_1(\cos\,\theta_\pi^*) + D_2' P_2(\cos\,\theta_\pi^*), \tag{7}$$

where $P_l(\cos\,\theta_\pi^*)$ is the l^{th}-order Legendre polynomial and D_l' is the corresponding Legendre moment. For single-pion

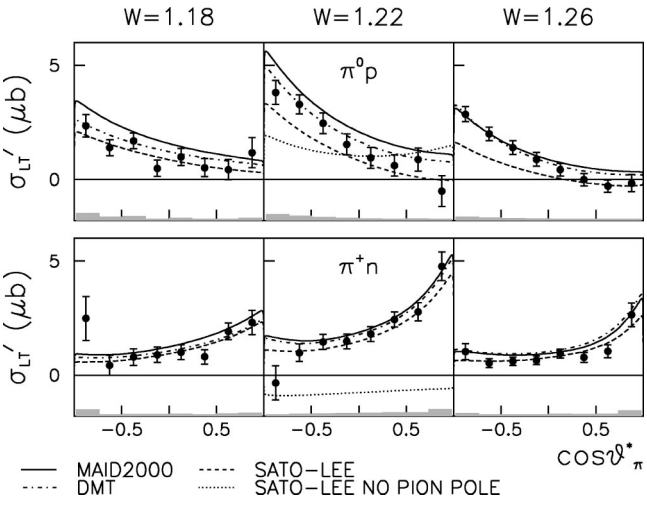

FIG. 3. CLAS measurements of $\sigma_{LT'}$ vs $\cos\,\theta_\pi^*$ for the $\pi^0 p$ channel [12] (top) and for the $\pi^+ n$ channel (bottom) extracted at $Q^2=0.40$ GeV^2 and $W=1.18-1.26$ GeV. The curves show model predictions discussed in the text. The shaded bars show estimated systematic errors.

electroproduction, each moment can be written as an expansion in magnetic ($M_{l_\pi^\pm}$), electric ($E_{l_\pi^\pm}$), and scalar ($S_{l_\pi^\pm}$) πN multipoles [22],

$$D_0' = -\,\mathrm{Im}[(M_{1-} - M_{1+} + 3E_{1+})^* S_{0+} + E_{0+}^*(S_{1-} - 2S_{1+}) + \ldots] \tag{8}$$

$$D_1' = -\,6\,\mathrm{Im}[(M_{1-} - M_{1+} + 3E_{1+})^* S_{1+} + E_{1+}^*(S_{1-} - 2S_{1+}) + \ldots] \tag{9}$$

$$D_2' = -\,12\,\mathrm{Im}[(M_{2-} - E_{2-})^* S_{1+} + \ldots], \tag{10}$$

where the πN angular momentum l_π combines with the nucleon spin to give the total angular momentum $J = l_\pi \pm 1/2$. The expansion for $D_{0,1}'$ is truncated at $l_\pi=1$, since s,p-wave interference terms involving the resonant multipoles M_{1+} and S_{1+} dominate at the peak of the $\Delta(1232)$. For D_2', model predictions for the π^0 channel are dominated by the $l_\pi=2$ multipoles shown in Eq. (10), while higher-order terms are important for the π^+ channel.

Figure 4 shows the model predictions for the Q^2 dependence of the Legendre moments at $W=1.22$ GeV compared to our measurements at $Q^2=0.4$ and 0.65 GeV^2. In contrast to our previous result for $D_0'(\pi^0 p)$ [12], which strongly disagreed with the MAID2000 and SL predictions, our result for $D_0'(\pi^+ n)$ is much closer to those models. The model variation is less pronounced, although the SL curve is still lower than the rest, due to the much smaller S_{0+} multipole in this model. Good agreement occurs for $D_1'(\pi^+ n)$, where there is almost no model dependence in the predictions. In contrast, $D_1'(\pi^0 p)$ shows more model dependence, with our measurement favoring MAID2000. For D_2', our results are consistent with the model predictions in sign and overall magnitude, although with large statistical errors.

The published electroproduction database is undergoing analysis by several groups in order to better determine the Q^2 dependence of the resonant multipoles which contribute to Eqs. (8)–(10). The MAID2003 fit [23] includes recent π^0 electroproduction data from Mainz, Bates, Bonn, and JLAB, while the more comprehensive SAID analysis [24] includes all previously published π^0 and π^+ data. Finally, the unitary isobar model (UIM) of Aznauryan [25] was fitted solely to the CLAS π^0 and π^+ electroproduction data (including the current polarization data) at $Q^2=0.4$ and 0.65 GeV^2. Figure 5 shows these fits compared to the W dependence of the measured Legendre moments, D_0' and D_1'.

The UIM fits show the best overall agreement with the $\sigma_{LT'}$ data, especially in the $\pi^+ n$ channel, while MAID2003 still overpredicts $D_0'(\pi^0 p)$. This may be due to the lack of polarization data in the global MAID fit. However, the UIM fit also overshoots $D_0'(\pi^0 p)$ slightly below the $\Delta(1232)$. The SAID XF18/SM01 solution [26] shows a somewhat different W dependence compared to the isobar models, which may reflect the different method of unitarization used in the SAID approach.

To explore the sensitivity of this polarization observable to backgrounds, we turned off various Born terms in the UIM calculation. First, we found that vector-meson ex-

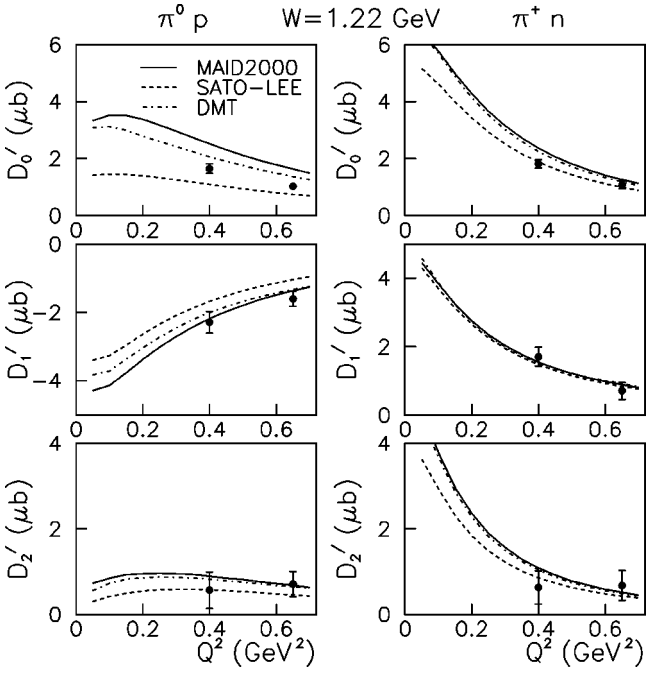

FIG. 4. The Q^2-dependence of Legendre moments of $\sigma_{LT'}$ for the $\pi^0 p$ channel [12] (left) and $\pi^+ n$ channel (right). The curves show model predictions described in the text. The data points are CLAS measurements showing statistical errors only.

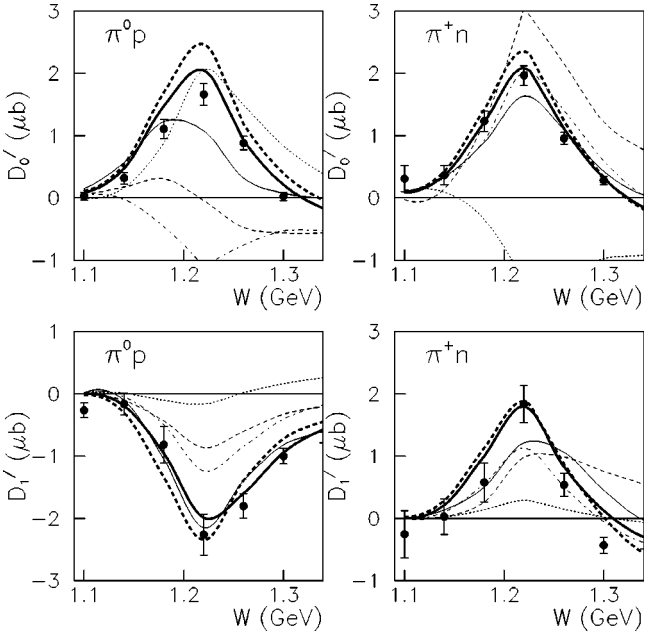

FIG. 5. The W dependence of $\sigma_{LT'}$ Legendre moments D_0' and D_1' for $\pi^0 p$ [12] (left) and $\pi^+ n$ (right) at $Q^2 = 0.40$ GeV^2. The bold curves show isobar model fits: UIM (solid), MAID2003 (dashed). The solid thin curve shows the SAID XF18/SM01 fit. The other curves show the UIM with the electric (dashed), magnetic (dot-dashed), and pion pole (dotted) Born terms turned off.

change had only a small ($<10\%$) effect on the magnitude of $\sigma_{LT'}$. On the other hand, as shown in Fig. 5, the $\pi^+ n$ channel is strongly sensitive to the t-channel pion pole term, while $D_0'(\pi^0 p)$ is similarly affected by the s- and u-channel electric and magnetic Born diagrams. Therefore, small adjustments to the hadronic form factors or meson couplings for these diagrams can affect the fits. The t-channel pion pole diagram is surprisingly important for $D_0'(\pi^0 p)$, where it strongly affects the phases of the S_{1+} and E_{1+} multipoles [13] which are responsible for much of the predicted backward peaking in Fig. 3. This was also verified by turning off the pole term in the SL model (dotted curve in Fig. 3). Note the pion pole can only influence the $\pi^0 p$ channel as a rescattering correction [14] via $\pi^+ n \to \pi^0 p$, which is introduced using the K-matrix method in UIM and MAID, or through an explicit meson-exchange potential in dynamical models.

The generally good agreement of the UIM fits to both our π^+ and π^0 data suggests that the K-matrix method of unitarizing the Born terms provides a consistent description of the backgrounds in the $\Delta(1232)$ region. More polarization data is needed at lower Q^2, which will allow further study of the $D_0'(\pi^0 p)$ term in a region where model sensitivity to pion rescattering is greatest.

We acknowledge the efforts of the staff of the Accelerator and Physics Divisions at Jefferson Lab in their support of this experiment. This work was supported in part by the U.S. Department of Energy and National Science Foundation, the Emmy Noether Grant from the Deutsche Forschungsgemeinschaft, the French Commissariat a l'Energie Atomique, the Italian Istituto Nazionale di Fisica Nucleare, and the Korea Research Foundation. The Southeastern Universities Research Association (SURA) operates the Thomas Jefferson Accelerator Facility for the United States Department of Energy under Contract No. DE-AC05-84ER40150.

[1] R. Beck *et al.*, Phys. Rev. Lett. **78**, 606 (1997).
[2] G. Blanpied *et al.*, Phys. Rev. Lett. **79**, 4337 (1997).
[3] V. V. Frolov *et al.*, Phys. Rev. Lett. **82**, 45 (1999).
[4] C. Mertz *et al.*, Phys. Rev. Lett. **86**, 2963 (2001).
[5] K. Joo *et al.*, Phys. Rev. Lett. **88**, 122001 (2002).
[6] N. Sparveris *et al.*, Phys. Rev. C **67**, 058201 (2003).
[7] G. Warren *et al.*, Phys. Rev. C **58**, 3722 (1998).
[8] T. Pospischil *et al.*, Phys. Rev. Lett. **86**, 2959 (2001).
[9] P. Bartsch *et al.*, Phys. Rev. Lett. **88**, 142001 (2002).
[10] C. Kunz *et al.*, Phys. Lett. B **564**, 21 (2003).
[11] A. Biselli *et al.*, Phys. Rev. C **68**, 035202 (2003).
[12] K. Joo *et al.*, Phys. Rev. C **68**, 032201 (2003).
[13] G. v. Gehlen, Nucl. Phys. **B26**, 141 (1970).
[14] R. L. Crawford, Nucl. Phys. **B28**, 573 (1971).
[15] B. Mecking *et al.*, Nucl. Instrum. Methods Phys. Res. A **503**, 513 (2003).
[16] A. Afanasev, I. Akushevich, V. Burkert, and K. Joo, Phys. Rev. D **66**, 074004 (2002).

[17] H. Egiyan, Ph.D thesis, William and Mary, 2001.
[18] T. Sato and T.-S. Lee, Phys. Rev. C **63**, 055201 (2001).
[19] S. S. Kamalov and S. N. Yang, Phys. Rev. Lett. **83**, 4494 (1999).
[20] D. Drechsel *et al.*, Nucl. Phys. **645**, 145 (1999).
[21] R. Arndt, W. Briscoe, I. Strakovsky, R. Workman, and M. Pavan, Phys. Rev. C **69**, 035213 (2004).
[22] A. S. Raskin and T. W. Donnelly, Ann. Phys. (N.Y.) **191**, 78 (1989).
[23] L. Tiator *et al.*, nucl-th/0310041.
[24] R. Arndt, I. Strakovsky, and R. Workman, nucl-th/0110001.
[25] I. G. Aznauryan, Phys. Rev. C **67**, 015209 (2003).
[26] R. Arndt and I. Strakovsky (private communciation).